The Morphology of Proximal Pole Scaphoid Fractures: Implications for Optimal Screw Placement

Timothy J. Luchetti, Youssef Hedroug, John J. Fernandez, Mark S. Cohen and Robert W. Wysocki

Abstract

The purpose of this study was to measure the radiographic parameters of proximal pole scaphoid fractures, and calculate the ideal starting points and trajectories for antegrade screw insertion. Computed tomography scans of 19 consecutive patients with proximal pole fractures were studied using open source digital imaging and communications in medicine (DICOM) imaging measurement software. For scaphoid sagittal measurements, fracture inclination was measured with respect to the scaphoid axis. The ideal starting point for a screw in the proximal pole fragment was then identified on the scaphoid sagittal image that demonstrated the largest dimensions of the proximal pole, and hence the greatest screw thread purchase. Measurements were then taken for a standard screw trajectory in the axis of the scaphoid, and a trajectory that was perpendicular to the fracture line. The fracture inclination in the scaphoid sagittal plane was 25 (SD10) °, lying from proximal palmar to dorsal distal. The fracture inclination in the coronal plane was 9 (SD16) °, angling distal radial to proximal ulnar with reference to the coronal axis of the scaphoid. Using an ideal starting point that maximized the thread purchase in the proximal pole, we measured a maximum screw length of 20 (SD 2) mm when using a screw trajectory that was perpendicular to the fracture line. This was quite different from the same measurements taken in a trajectory in the axis of the scaphoid. We also identified a mean distance of approximately 10 mm from the dorsal fracture line to the ideal starting point. A precise understanding of this anatomy is critical when treating proximal pole scaphoid fractures surgically.

Keywords

Proximal pole, scaphoid fracture, computed tomography, internal fixation, cannulated screw

Introduction

Scaphoid fractures are typically classified by morphology and location. Although distal pole and waist fractures are most common, it is the proximal pole variant that is most difficult to treat. These proximal pole injuries represent 6–20% of all scaphoid fractures (Eastley et al., 2013; Gholson et al., 2011; Kawamura and Chung, 2008; Margo and Seely, 1963; Stewart, 1954).

The difficulty of achieving union in proximal pole fractures is multifactorial. This area of the bone is poorly vascularized (Steinmann and Adams, 2006). In addition, the small proximal fragment makes internal fixation more difficult. Reported union rates for non-operative management of these injuries have ranged from 5% to 90% (Gholson et al., 2011; Grewal et al., 2016; Margo and Seely, 1963; Steinmann and Adams, 2006). In a meta-analysis of 1147 acute

scaphoid fractures, Eastley et al. (2013) found a 34% nonunion rate with immobilization alone. When compared to more distal fractures treated with immobilization, they showed a relative risk of 7.5 for the development of a symptomatic nonunion.

Although there is controversy about surgical indications for non-displaced proximal pole injuries (Grewal et al., 2016), open reduction and internal fixation is often preferred. Most commonly, an antegrade headless screw is used for this purpose

Department of Orthopedic Surgery, Rush University Medical Center, Chicago, IL, USA

Corresponding author:
Timothy J. Luchetti, MD Department of Orthopedic Surgery, Rush University Medical Center, 1611 West Harrison Street, Chicago, IL 60612, USA.
Email: tjluke25@gmail.com

(Gholson et al., 2011). Research efforts to date have focused on scaphoid bone morphology (Kong et al., 2009), the optimal design of the compression screw (Crawford et al., 2012) and refinement of the reduction technique (Haisman et al., 2006; Kawamura and Chung, 2008). Studies comparing screw trajectories have focused mainly on scaphoid waist and distal pole fractures.

The purposes of this study were: to describe radiographic parameters of proximal pole scaphoid fracture morphology; to describe the ideal starting point for an antegrade screw that would maximize purchase in the proximal fragment; and to determine the maximum screw lengths for a screw trajectory perpendicular to the fracture line versus one in the axis of the scaphoid. We hypothesized that the two trajectories would be different, and lead to different maximum screw length.

Methods

After obtaining Internal Review Board (IRB) approval, a retrospective review of skeletally-mature patients who presented to our institution with an acute scaphoid fracture was carried out. All patients had computed tomography (CT) imaging using 0.5 mm contiguous cuts. Reformatted images in the sagittal and coronal plane in the long axis of the scaphoid were used for measurements (i.e. ''scaphoid sagittal,'' Figure 1). All scaphoid waist or distal pole fractures were excluded, leaving only proximal pole scaphoid fractures, defined as a fracture line in the proximal one-fourth of the scaphoid (measured along

Figure 1. Coronal 'scout' image with grid overlay centred along the long axis of the scaphoid bone for reconstruction of scaphoid sagittal computed tomography view.

its long axis on the central scaphoid sagittal image). Between December 2009 and March 2015, 19 patients met the above criteria and were included in the study.

To assess fracture morphology, two independent reviewers assessed the pre-operative CT imaging. All CT imaging was imported to an open source digital imaging and communications in medicine (DICOM) imaging measurement software known as Horos (www.horosproject.org). Although Horos is not specifically approved by the Food and Drug Administration (FDA), it is in common use. All subsequent measurements were made using a grid measurement system within the Horos program.

The size of the proximal pole fragment was determined from both the scaphoid sagittal and coronal images. Specifically, the height of each proximal pole fragment was measured on the slice in a given series with the greatest depth of bone visible, and the width of the bone measured at the fracture site on the view where the fracture appeared the widest. The greatest value of either the coronal or scaphoid sagittal values was used for both height and width. In addition, the fragment size was measured as a percentage of the overall length of the bone, as viewed on the largest sagittal scaphoid CT slice.

For measurements on the coronal CT cuts, based on a coordinate system defined by the radius, the axis of the scaphoid was drawn as a line through the midpoints of the proximal and distal poles. This line was created by transposition from the CT slice that showed the most proximal extent of the proximal pole, onto the CT slice that showed the most distal extent of the distal pole. Once this line had been generated, it was transposed to the CT slice that most clearly defined the direction of the fracture line. The angle between the coronal scaphoid axis and the fracture line was then calculated (Figure 2). With respect to the coronal scaphoid axis, positive (+) measurements denote a fracture coursing from distal radial to proximal ulnar (radial inclination), whereas negative (−) measurements denote a fracture coursing from distal ulnar to proximal radial (ulnar inclination).

A variation of this methodology was used for measurements of the scaphoid sagittal CT views. The axis of the scaphoid was defined as a line that was traced along the most ventral points of the proximal and distal poles (scaphoid sagittal axis). This line was created by transposition from the CT slice that showed the most proximal extent of the proximal pole, onto the CT slice that showed the most distal extent of the distal pole. The scaphoid sagittal axis was then transposed to the CT slice that most accurately depicted the major fracture line through the scaphoid. The angle between the scaphoid sagittal

axis and the fracture line was then calculated (Figure 3). A positive (+) measurement denotes a fracture line coursing from proximal dorsal to palmar distal (i.e., 'extended'), whereas a negative (−) measurement denotes a fracture line coursing from proximal volar to distal dorsal (i.e., 'flexed').

Figure 2. Fracture inclination as measured on the coronal computed tomography view.

The ideal starting point for a screw in the proximal pole fragment was then identified on the scaphoid sagittal image that demonstrated the largest dimensions of the proximal pole, and hence the greatest screw thread purchase. The Horos software allows the user to measure the perimeter along a curve, making these measurements easy to perform. The ideal starting point was identified as the point along the curve of the articular surface with the largest depth from the fracture line, based on a perpendicular line extending proximally from the fracture line (Figure 3).

The maximum lengths of a screw parallel to the scaphoid sagittal axis (i.e., 'sagittal axis screw'; Figure 4) and a screw perpendicular to the fracture line (i.e., 'eccentric screw'; Figure 5) were then calculated. To avoid violating the cortical surface, we used a 'safe zone' of 2 mm of bone on the dorsal and volar sides of the projected screw trajectory, which would accommodate most systems used today. This number is similar to a study by Leventhal et al. (2009) in which a 2.3 mm cutoff was recommended.

The maximum screw lengths along each axis were measured from the proximal inner cortical surface to the distal inner cortical surface, to avoid screw penetration of the cortex. The distance between the ideal starting point of the eccentric screw trajectory and the starting point of the sagittal axis screw trajectory was measured along the perimeter of the proximal fragment.

Similar methods were used to assess the available length for screw placement in the coronal CT view. First, the coronal slice that best showed the fracture plane was used to define the line perpendicular to the
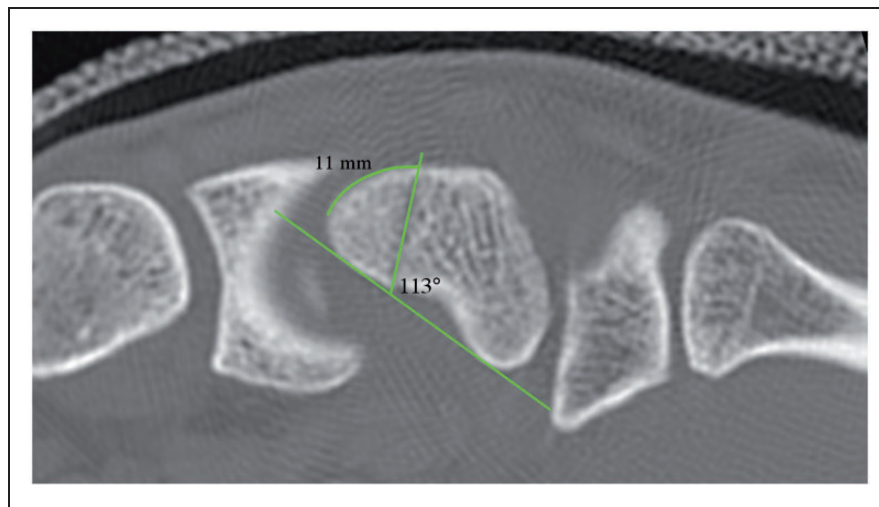
Figure 3. Fracture inclination and ideal start point as measured on scaphoid sagittal computed tomography view. A line that is tangent to the volar tubercles of both poles defines the scaphoid axis.
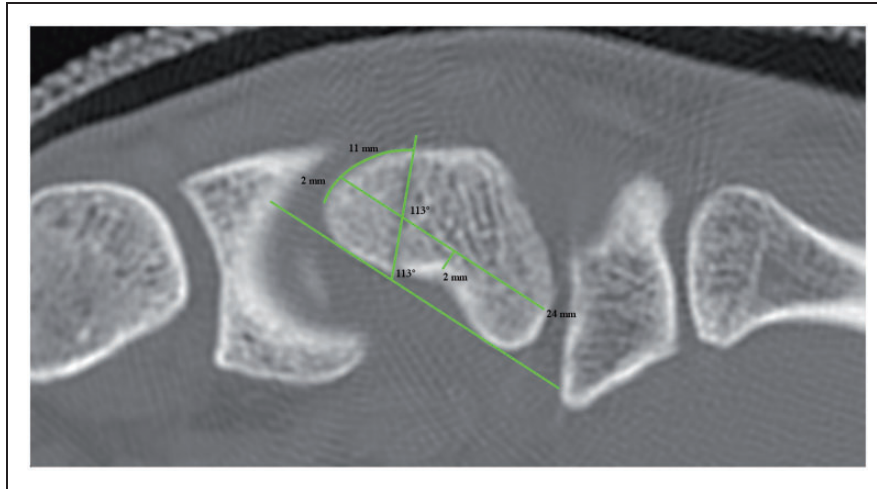
Figure 4. Maximum screw length for scaphoid axis trajectory as measured on the scaphoid sagittal computed tomography view. A minimum 'safe zone' of 2 mm is applied to avoid cortical breach. Note the measured distance of 2 mm representing the location of the starting point in relation to the ideal starting point, which is dictated by the minimum 'safe space' of 2 mm necessary to avoid cortical breach. In this case, the screw is closest to the volar cortex at roughly the mid-waist, and 24 mm of bone is available for a screw in this trajectory.
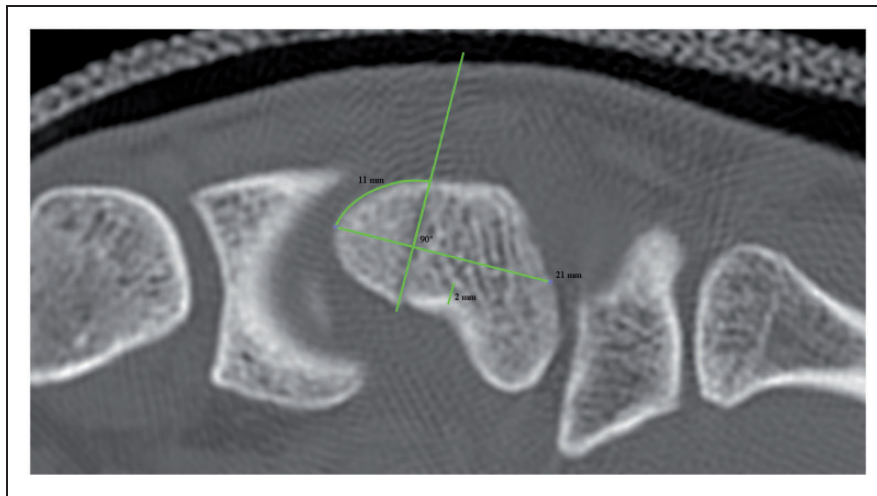
Figure 5. Maximum screw length for eccentric trajectory as measured on scaphoid computed tomography view. Note that the 2 mm safe zone has no effect on screw position. The start point coincides with the ideal position for this trajectory. 21 mm of bone is available for this screw trajectory.

fracture plane. Once this axis was determined, a 2 mm line representing the 'safe zone' was created in parallel with the fracture line. This line was then projected onto every coronal CT slice to define the 'narrowest' portion of the scaphoid. The axis was then translated such that the full 2 mm of bone was present on either side of the line on every coronal CT slice. The axis was then transposed to the coronal slice in which the proximal extent of the proximal

pole was visible. The line was shortened or lengthened such that it abutted the inner cortex of the proximal pole. The same method was then used to approximate the inner cortex of the distal pole on its appropriate CT slice. By aligning the two slices, the length of the corridor of bone available for an eccentric screw was measured. Finally, a conservative estimate of the length available for a screw perpendicular to the fracture line was

calculated. In each individual, the minimum screw length was obtained by considering both the coronal and scaphoid sagittal CT measurements. Descriptive statistics were given as means and standard deviations for continuous variables. Two-tailed unpaired Student's *t*-tests were used to compare continuous variables in equal groups, and significance was set at $p \leq 0.05$.

Results

There were 18 men and one woman; the mean age was 22 years (range, 14–34). All injuries were the result of low energy trauma, typically from a ground level fall or a sports injury. There was no evidence of pre-existing arthrosis or deformity in any patients in this series. The mean dimensions of the proximal pole fragments were 6×6 mm at their greatest depth from the fracture line on orthogonal views. The mean length of the proximal pole fragment was 22% (range, 13–25) of the scaphoid length.

Based on coronal CT views, the mean fracture inclination was 9 (SD 16) ° of radial inclination. When measurements of length available for the eccentric screw were taken, the radial cortex was not 'at risk' for cortical breach in any case. However, the ulnar cortex was deemed 'at risk' in a number of cases. Typically, this area occurred somewhere near the mid-waist. When this occurred, the screw axis was translated in the radial direction until 2 mm of bone was available ulnarly on every coronal slice, which led to shorter screw lengths. The mean length available for a screw placed perpendicular to the fracture line was 22 (SD 2) mm on the coronal CT views. On the scaphoid sagittal views, the mean fracture inclination was extended +25 (SD 10) ° in reference to the sagittal axis of the scaphoid (Table 1). The ideal starting point for an antegrade screw was 10 (SD 2) mm proximal to the fracture line along a curve measured along the dorsal perimeter of the proximal fragment. When the eccentric screw starting point and the ideal starting point were the same, the sagittal axis screw trajectory was outside of the safe zone in 15 of 19 cases and necessitated a more dorsal starting point, 2 (SD 1) mm away (Table 2).

When the minimum screw length available from both coronal and scaphoid sagittal CT slices were considered for each individual, the mean screw length for a screw placed perpendicular to the fracture line was 20 (SD 2) mm. The mean length of a scaphoid axis screw was 25 (SD 2) mm. The maximum length available for the sagittal axis screw was significantly greater than for the eccentric screw

Table 1. Fracture inclination on two different computed tomographic views of trajectories.

	CT view	Mean (°)	SD (°)
Fracture inclination	Coronal*	9	16
Fracture inclination	Sagittal scaphoid*,§	25	10

*For sagittal scaphoid views, positive (+) measurements denote 'extension' of the fracture line relative to the long axis of the scaphoid, whereas negative (−) measurements denote 'flexion'. For coronal views, positive (+) measurements denote 'radial inclination' of the fracture line relative to the long axis of the scaphoid, whereas negative (−) measurements denote 'ulnar inclination'.
§Scaphoid view denotes a view centred along the long axis of the scaphoid bone.
CT: computed tomography; SD: standard deviation; mm: millimetres.

Table 2. Distance to ideal start point for eccentric and scaphoid axis screw trajectories.

Eccentric trajectory (mm) Mean (SD)	Scaphoid axis trajectory (mm) Mean (SD)
0 (0)	2 (1)

based on the sagittal axis CT measurements ($p < 0.001$).

Discussion

Central screw placement along the axis of the scaphoid leads to optimal stability (McCallister et al., 2003) and high union rates (Trumble et al., 2000) for scaphoid waist fractures. For proximal pole fractures, the optimal screw orientation has not been established. Several authors have suggested that screw placement perpendicular to the fracture line may optimize healing of proximal pole fractures, by increasing stability (Luria et al., 2015) and by minimizing the risk of comminution of the proximal pole (Hart et al., 2013). There is currently little information on the typical morphology of this fracture variant to guide surgeons.

Through CT evaluation of 19 patients, we found wide variability with respect to fracture inclination in the coronal plane, with the fracture usually being radially inclined relative to the long axis of the radius (Table 1). In the sagittal plane, we consistently observed that proximal pole fracture morphology was dorsally inclined relative to the scaphoid long axis. In other words, all fractures began more

proximally on the dorsal side and exited more distally on the palmar side of the bone.

Although using measurements on two-dimensional CT images has some limitations, we defined the optimal starting position and the mean screw length with fixation directed perpendicular to the fracture line. This theoretically maximizes thread purchase in the proximal fragment. A screw trajectory perpendicular to the fracture line also neutralizes shear forces that can lead to fracture displacement (Hart et al., 2013). We have shown that the sagittal axis trajectory precludes the use of the ideal starting point in most cases owing to the risk of breaching the volar cortex. However, moving the starting point dorsally in the proximal pole away from the ideal starting point, in an effort to avoid a volar cortical breach at the waist, may lead to less proximal pole bone being available for thread purchase and compromise fixation in the proximal pole.

When considering the coronal plane, an eccentric screw trajectory produced a similar problem. The ulnar cortex, with its concave shape, was found to be 'at risk' for cortical breach in a number of cases. Fortunately, this trajectory in the coronal plane is easier to assess intraoperatively through a dorsal approach to the wrist with fluoroscopy. As such, the starting point for the screw may need to be adjusted slightly more radial to the ideal starting point to avoid this complication.

The ideal starting point in the sagittal plane may be more difficult to identify during surgery. To gain access to the thickest part of the proximal pole fragment, the wrist needs to be maximally flexed. Carpal bone overlap on a lateral radiographic makes visualization of this area difficult. For these smaller, more proximal pole injuries, we believe that the more volar screw starting position is particularly critical.

The eccentric trajectory that we propose starts at the thickest portion of the proximal pole fragment to provide the optimal screw purchase. It may potentially be biomechanically superior to maximize thread purchase in the proximal pole and compression across the fracture by starting the screw at the ideal position by using a trajectory that is angled toward the dorsal cortex and not down the true bone axis. For the sake of simplicity, a distance of approximately 10 mm proximal to the dorsal fracture line can be used as a reference point in these injuries for the typical distance. However, each fracture is unique. The starting point and distance from the fracture line should be measured preoperatively on the true sagittal long axis CT slice in each case.

When placing the screw perpendicular to the fracture, it is important to understand that this will lead to a shorter maximum length screw than central placement. In the scaphoid sagittal plane, an eccentric screw will be directed toward the dorsal cortex of the bone and thus reach its limit sooner than if it is placed more palmarly along the sagittal axis. Whilst the risk of ulnar cortical perforation is possible in the coronal plane, we again feel that this can be avoided intraoperatively with close attention to fluoroscopy. Eccentric placement does have the theoretical disadvantage of having fewer screw threads distal to the fracture, but distal purchase is not typically a problem in these proximal pole injuries. As such, we believe that a shorter screw is a justified trade-off, since purchase in the proximal fragment is optimized with this technique.

In their study of 50 cadaveric scaphoid bones, Compson et al. (1994) recognized three morphologic variants of this oddly-shaped bone. One variant involved an under-developed proximal pole. If encountered, this shape would have implications for screw placement. The uniformly convex-shaped proximal pole in this series did not confirm the 'cone-shaped' proximal pole morphology described by Heinzelmann et al. (2007). A line drawn starting at the tip of the proximal pole passed through the fracture line in a perpendicular fashion, with adequate screw purchase and avoidance of screw prominence in each specimen. It is important, however, that by the use of pre-operative CT imaging the surgeon recognizes any morphological variation in each individual patient, and plans accordingly for fixation.

One limitation of this study is the small number of patients. The clinical benefit of an 'ideal' starting point and eccentric screw trajectory will need to be established in a larger series of patients. Another limitation is the relatively uniform fracture configuration in our series; there were no comminuted or high-energy fractures that presented during the study period. The Horos software is not essential to the identification and measurement of 'eccentric' and 'long axis' trajectories or the 'ideal' starting point, which can be identified on coronal and sagittal reformatted computed tomographic images with most picture archiving and communication systems (PACS). Finally, we used a two-dimensional analysis of a complex three-dimensional structure. We believe, however, that this approach is accurate and more clinically useful to the surgeon than a three-dimensional analysis, which may be unavailable at some centres.

In summary, we have identified the typical proximal pole fracture orientation in the coronal and sagittal planes. Of note, these fractures are consistently 'extended' in the sagittal plane. This makes the optimal screw length, trajectory and starting point

potentially different from those that are used in waist fractures. We report an ideal starting point to maximize thread purchase in the small proximal pole. Screw placement perpendicular to the fracture line in the sagittal plane results in a shorter screw length as opposed to screw placement in the scaphoid sagittal axis, which results in a starting point closer to the dorsal fracture line, and which may risk comminution during insertion.

Declaration of conflicting interests The authors declared no potential conflicts of interest with respect to the research, authorship, and/or publication of this article.

Funding The authors received no financial support for the research, authorship, and/or publication of this article.

References

Compson JP, Waterman JK, Heatley FW. The radiological anatomy of the scaphoid. Part 1: Osteology. J Hand Surg Br. 1994, 19: 183–7.

Crawford LA, Powell ES, Trail IA. The fixation strength of scaphoid bone screws: an in vitro investigation using polyurethane foam. J Hand Surg Am. 2012, 37: 255–60.

Eastley N, Singh H, Dias JJ, Taub N. Union rates after proximal scaphoid fractures; meta-analyses and review of available evidence. J Hand Surg Eur. 2013, 38: 888–97.

Gholson JJ, Bae DS, Zurakowski D, Waters PM. Scaphoid fractures in children and adolescents: contemporary injury patterns and factors influencing time to union. J Bone Joint Surg Am. 2011, 93: 1210–9.

Grewal R, Lutz K, MacDermid JC, Suh N. Proximal pole scaphoid fractures: a computed tomographic assessment of outcomes. J Hand Surg Am. 2016, 41: 54–8.

Haisman JM, Rohde RS, Weiland AJ. Acute fractures of the scaphoid. J Bone Joint Surg Am. 2006, 88: 2750–8.

Hart A, Mansuri A, Harvey EJ, Martineau PA. Central versus eccentric internal fixation of acute scaphoid fractures. J Hand Surg Am. 2013, 38: 66–71.

Heinzelmann AD, Archer G, Bindra RR. Anthropometry of the human scaphoid. J Hand Surg Am. 2007, 32: 1005–8.

Kawamura K, Chung KC. Treatment of scaphoid fractures and nonunions. J Hand Surg Am. 2008, 33: 988–97.

Kong WY, Xu YQ, Wang YF, Chen SC, Liu ZL, Li XG. Anatomic measurement of wrist scaphoid and its clinical significance. Chin J Traumatol. 2009, 12: 41–4.

Leventhal EL, Wolfe SW, Walsh EF, Crisco JJ. A computational approach to the ''optimal'' screw axis location and orientation in the scaphoid bone. J Hand Surg Am. 2009, 34: 677–84.

Luria S, Schwarcz Y, Wollstein R, Emelife P, Zinger G, Peleg E. 3-dimensional analysis of scaphoid fracture angle morphology. J Hand Surg Am. 2015, 40: 508–14.

Margo MK, Seely JA. A statistical review of 100 cases of fracture of the carpal navicular bone. Clin Orth Rel Res. 1963, 31: 102–5.

McCallister WV, Knight J, Kaliappan R, Trumble TE. Central placement of the screw in simulated fractures of the scaphoid waist: a biomechanical study. J Bone Joint Surg Am. 2003, 85-A: 72–7.

Steinmann SP, Adams JE. Scaphoid fractures and nonunions: Diagnosis and treatment. J Orthop Sci. 2006, 11: 424–31.

Stewart MJ. Fractures of the carpal navicular (scaphoid); a report of 436 cases. J Bone Joint Surg Am. 1954, 36: 998–1006.

Trumble TE, Gilbert M, Murray LW, Smith J, Rafijah G, McCallister WV. Displaced scaphoid fractures treated with open reduction and internal fixation with a cannulated screw. J Bone Joint Surg Am. 2000, 82: 633–41.